

# Constraining modified gravity models through strong lensing cosmography

Mario H. Amante, Andrés Lizardo,<sup>\*</sup> Javier Chagoya, and C. Ortiz

*Unidad Académica de Física, Universidad Autónoma de Zacatecas, C.P. 98060, Zacatecas, México.*

(Dated: March 18, 2024)

We analyze cosmography as a tool to constrain modified gravity theories. We take four distinct models and obtain their parameters in terms of the cosmographic parameters favored by observational data of strong gravitational lensing. We contrast with the values obtained by direct comparison between each model and the observational data. In general, we find consistency between the two approaches at  $2\sigma$  for all models considered in this work. Our study bridges the gap between theoretical predictions of modified gravity and empirical observations of strong gravitational lensing, providing a simple methodology to test the validity of these models.

## I. INTRODUCTION

A revolution in cosmology began when observational data, such as Type Ia supernovae [1], revealed that the universe is currently undergoing a phase that appears to involve accelerated expansion of spacetime. Amongst the many efforts to explain this accelerated expansion, the most accepted proposal is the  $\Lambda$ CDM model, also known as the standard cosmological model, which considers that the constituents of the Universe, in addition to those dictated by the standard model of particle physics, are cold dark matter (CDM) and a cosmological constant ( $\Lambda$ ) that is responsible for the present day expansion of the Universe. This model is consistent with cosmic microwave background (CMB) physics [2] and large scale structure observations [3, 4]. However, recent measurements indicate some tension between different estimations of both the Hubble constant  $H_0$  and the  $S_8$  parameter, depending on whether these are based on the CMB or on measurements in the nearby Universe. These enduring and persistent tensions display disparities of up to  $6\sigma$  for  $H_0$  and around  $3\sigma$  for the  $S_8$  parameter when some dataset are considered (see [5, 6] for an extensive analysis). Furthermore, there is a long standing theoretical issue with the  $\Lambda$ CDM model. If  $\Lambda$  is interpreted as vacuum energy, then Quantum Field Theory predicts a value for  $\Lambda$  that deviates from the observational value by several orders of magnitude. These anomalies have been part of the motivation to formulate alternative explanations for the gravitational behavior of our Universe. These alternatives comprise an extensive range of possibilities, broadly divided into those that alter the energy-momentum tensor and those that modify the geometrical component of the Einstein equations; see, for example, [7–9]. Apart from satisfying certain theoretical requirements, these alternative theories should be tested through comparison with observational data, which constantly improve in their precision.

Rather than testing alternatives to GR and  $\Lambda$ CDM on a model-by-model basis, it is convenient to have a framework to analyze the dynamics of the universe without any assumptions on the underlying model of gravity. This is the foundation of cosmography, which analyzes the Hubble factor in a Taylor expansion around the present time. The coefficients of the expansion – so called cosmographic parameters – are related to the derivatives of the scale factor at the present time. The goal is thus to derive the values of the cosmographic parameters from local observations. Several analyses on the usefulness of cosmography as a model independent test of gravity have been reported in the literature (e.g. [10, 11]). A modification of the method that has attracted some attention is dubbed  $y$ -redshift, which provides the theoretical advantage of mapping the redshift  $z \in [0, \infty)$  to a parameter  $y \in [0, 1)$ . In a similar spirit, a logarithmic expansion was presented in [12]. These approaches have been used to estimate cosmographic parameters with different observational data sets (e.g. [13–16]).

In this work, we revisit the question of whether cosmography is a viable approach to reconstruct alternative models of cosmology. We focus on the use of an updated catalog of strong gravitational lenses (SLS, Strong Lensing Systems) [17] as a tool for constraining cosmological and cosmographic parameters. First, we obtain the best fit parameters for each model, then we perform some tests to analyse whether these models are compatible with cosmography, and finally we try to reconstruct the models starting from the best fit cosmographic parameters. Our methodology is based on a proposal for inferring cosmological parameters using elliptical galaxies as gravitational lenses [18], which has been extended in the literature to include various lensing systems at different scales [19–30]. It is also worth mentioning that lensing observations hold promise as a valuable tool for analyzing the distribution of dark matter in galaxies and populations of galaxies [31–34].

This work is organized as follows. In Sec. II we present the alternative cosmological models under consideration. In Sec. III, we present the data and methodology to be used to analyze the cosmological models using strong lensing

<sup>\*</sup> andres.lizardo@fisica.uaz.edu.mx

observations. We also discuss the methodology to assess the viability of cosmography for reconstructing alternative cosmological models with strong lensing systems. In Sec. IV, we report the constraints for the free parameters of each model, and we also present the novel contrast with cosmography. In Sec. V we give our concluding remarks and discuss some possibilities for future studies.

## II. MODELS OF BACKGROUND COSMOLOGY

In this section we present the cosmological models to be used in order to assess the validity of cosmography for constraining cosmological parameters using gravitational lenses. These models come from different theoretical approaches, including the  $\omega$ CDM parametrization, a holographic inspired model (hFRW), a subset of degenerate higher order scalar tensor theories (DHOST), and a model that considers coupling between gravity and the energy-momentum tensor ( $f(R, T)$ )<sup>1</sup>.

### A. $\omega$ CDM

The  $\omega$ CDM model is an extension of  $\Lambda$ CDM where the equation of state for dark energy is constant, but can be different from  $\omega = -1$ . The equation of state should satisfy the condition  $\omega < -\frac{1}{3}$  to produce an accelerated expansion of the universe. The dimensionless Friedmann equation,  $E(z) = H(z)/H_0$ , for a Universe consisting of baryonic matter, cold dark matter, and dark energy parametrized by  $\omega$  can be written as

$$E(z)_{\omega CDM}^2 = \Omega_{0m}(1+z)^3 + (1 - \Omega_{0m})(1+z)^{3(1+\omega)}, \quad (1)$$

where  $\Omega_{0m}$  is the matter density parameter of baryonic and cold dark matter at  $z = 0$ . Also, we are considering a flat universe, and the constraint  $E(0) = 1$  has been imposed.

In the next section, we use the normalized Hubble parameter  $E(z)$  to obtain the angular diameter distance.

### B. hFRW

The holographic FRW (hFRW) model consists of a FRW brane embedded in a flat bulk with an extra dimension relative to the brane. In this model, the stress-energy tensor of dark matter and dark energy is determined by the holographic stress-energy tensor on the brane hypersurface [35]. The dimensionless Friedmann equation can be written as

$$E(z)_{hFRW} = \sqrt{\frac{\Omega_{0\lambda}}{2} + \Omega_{0B}(1+z)^3 + \frac{\Omega_{0\lambda}}{2} \left[ 1 + \frac{4\Omega_{0B}}{\Omega_{0\lambda}}(1+z)^3 + \frac{4\Omega_{0I}}{\Omega_{0\lambda}}(1+z)^4 \right]^{1/2}}, \quad (2)$$

where  $\Omega_{0\lambda}$  is the dark energy density parameter,  $\Omega_{0B}$  is the baryonic matter density parameter and  $\Omega_{0I}$  is a density parameter related with an integration constant  $I$  coming from the metric field equations in the hFRW scenario (see [35, 36] for details). Imposing the flatness condition  $E(0) = 1$ , we obtain  $\Omega_{0I} = (1 - \Omega_{0\lambda} - 2\Omega_{0B} + \Omega_{0B}^2) / \Omega_{0\lambda}$ . Using this constraint to reduce the number of free parameters, equation (2) becomes

$$E(z)_{hFRW} = \sqrt{\frac{\Omega_{0\lambda}}{2} + \Omega_{0B}(1+z)^3 + Q^{\frac{1}{2}}}, \quad (3)$$

where  $Q = \Omega_{0\lambda}^2/4 + \Omega_{0\lambda}\Omega_{0B}(1+z)^3 + (1 - \Omega_{0\lambda} - 2\Omega_{0B} + \Omega_{0B}^2)(1+z)^4$ . It is worth noting that in the case  $\Omega_{0I} = 0$  we recover the Friedmann equation of the self-accelerating branch of the Dvali-Gabadadze-Porrati model, which can also be obtained from entropic gravity (see [37] for details).

---

<sup>1</sup> Not to be confused with theories of gravity that consider torsion, usually denoted  $F(R, T)$ .

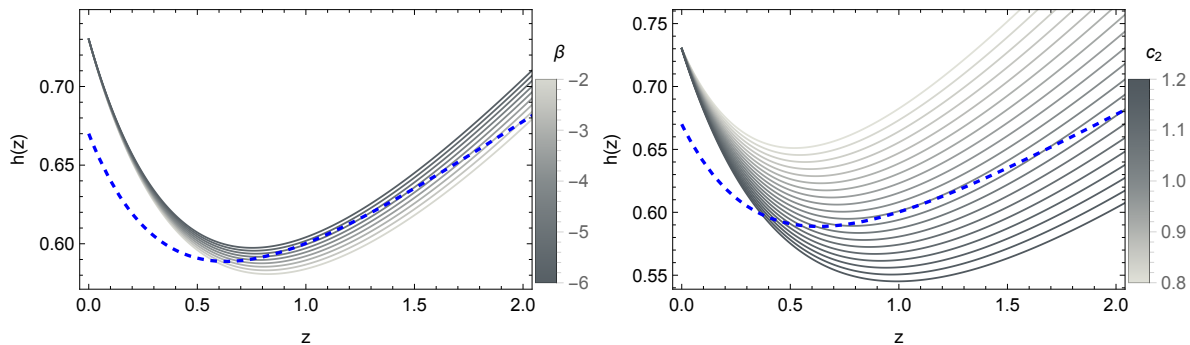


FIG. 1. Numerical solutions for the reduced Hubble parameter as a function of redshift. In the left panel, we fix  $c_2 = 1, c_3 = 5, c_4 = 1$  and  $\beta \in [-6, -2]$ , while in the right panel  $\beta = -5.3, c_3 = 5, c_4 = 1$  and  $c_2 \in [0.8, 1.2]$ .

### C. DHOST

Degenerate Higher Order Scalar-tensor Theories (DHOST) are a generalization of Horndeski gravity that allows for equations of motion of order higher than two, as long as a condition to avoid propagation of Ostrogradski instabilities is satisfied. We use a subsector of this theory that is compatible with luminal propagation of gravitational waves, and has been shown to admit scaling solutions that mimic matter domination at early times and dark energy domination at late times. The general solution for the Hubble parameter in this sector is obtained numerically [38] and depends on four<sup>2</sup> free parameters that appear in the free functions of the DHOST Lagrangians (see Appendix B for details). We constructed a set of solutions for several values of two of these parameters, named  $\beta$  – which parameterises the difference between DHOST and beyond Horndeski, and  $c_2$  – which is associated with the canonical kinetic term of the scalar field, while the remaining two parameters are arbitrarily fixed as  $c_3 = 5, c_4 = 1$ . Some examples of the profiles for  $H(z)$  are presented in Fig. 1.

### D. $f(R, T)$

The framework of  $f(R, T)$  gravity is an extension of GR which allows for matter-curvature coupling in the Universe. The action is defined as follows:

$$S = \int \left( \frac{f(R, T)}{16\pi G} + S_m \right) \sqrt{-g} dx^4, \quad (4)$$

where  $S_m$  is the action for matter,  $R$  the Ricci scalar and  $T$  the trace of the energy-momentum tensor associated to  $S_m$ . An exact cosmological solution under the assumption  $f(R, T) = \lambda(R+T)$  has been derived in [41], with  $\lambda$  an arbitrary coupling constant of  $f(R, T)$  gravity. The authors employ a parametrization<sup>3</sup> of the Hubble parameter compatible with the existence of accelerating and decelerating phases in the evolution of the Universe. The corresponding dimensionless Friedmann equation has the form

$$E(z) = \frac{1}{2} (1 + (1+z)^n), \quad (5)$$

where  $n$  is parameter related to the physical parameters of the  $f(R, T)$  scenario.

## III. DATA AND METHODOLOGY

Our methodology consists of two main steps: we show that the models under consideration are compatible with cosmography, and then we try to reconstruct them from the model independent cosmographic parameters. In the

<sup>2</sup> A fifth parameter,  $\Lambda_3$ , can be absorbed in a change of variables that makes the Hubble factor dimensionless. We account for this by normalizing the solution so that  $h_0 = 0.74$ , which is compatible with local observations [39, 40].

<sup>3</sup> The choice of this parametrization arises from the fact that, in  $f(R, T)$ , two independent equations are obtained in terms of three unknowns. Therefore, the parameter  $n$  constrained by the data is related to the physical parameters of the model.

first step, we take the dimensionless Friedmann equation for the models described in the previous sections, we fit their parameters using SLS, we compute their theoretically related cosmographic parameters, and we compare them with the actual, model independent, cosmographic parameters estimated from SLS. In the second step, we obtain the parameters of each model from the model independent cosmographic parameters, and compare to their actual best fits to SLS. In the following, we discuss the steps of our methodology in more detail.

### A. Data and estimation of cosmological parameters

We constrain the parameters of each of the models presented in the last section using observations from SLS. We use the fiduciary sample presented in [17] with a total of 143 systems. In addition, we use a sub-sample of 99 systems discussed in [13] which avoids nonphysical results when calculating the angular diameter distances in a Taylor series approximation, as required in cosmography<sup>4</sup>.

In the strong lensing phenomenon, the deflection of the light beam is so significant that it can lead to the formation of arcs, multiple images, or even Einstein rings. These images contain crucial properties that are valuable for modeling a lens system, thereby providing essential insights into various astrophysical phenomena. Consequently, observations of strong gravitational lensing play a pivotal role in analyzing the evolution of the Universe. We used early-type galaxies as gravitational lenses, considering four measured properties: spectroscopically determined stellar velocity dispersion  $\sigma$ , the Einstein radius  $\theta_E$ , the lens redshift  $z_l$ , and the source redshift  $z_s$ . Our approach involves a method that describes the mass distribution of the lens by correlating the separation between multiple images of the source with the angular diameter distances to the lens and the source. If the lens model fitted to the observed images is assumed to be a spherical mass distribution, described by a singular isothermal sphere (SIS) model, the Einstein radius is defined as [42]

$$\theta_E = 4\pi \frac{\sigma^2 D_{ls}}{c^2 D_s}, \quad (6)$$

where  $c$  represents the speed of light,  $D_s$  denotes the angular diameter distance to the source,  $D_{ls}$  stands for the angular diameter distance between the lens and source, and  $\sigma$  represents the measured velocity dispersion of the lensing galaxy. The mass distribution of elliptical galaxies is well described as isothermal, as indicated by previous studies [18, 43–46].

In any cosmological model, the angular diameter distance is defined as

$$D(z) = \frac{c}{H_0(1+z)} \int_0^z \frac{dz'}{E(z')}, \quad (7)$$

where  $H_0$  is the Hubble constant and  $E(z)$  is the dimensionless Friedmann parameter, presented in the previous section for the models of interest in this work. By defining the ratio  $D \equiv D_{ls}/D_s$ , the observational lens equation in the isothermal regime can be expressed as

$$D^{obs} = \frac{c^2 \theta_E}{4\pi \sigma^2}, \quad (8)$$

The theoretical counterpart is defined as follows

$$D^{th}(z_l, z_s; \Theta) = \frac{\int_{z_l}^{z_s} \frac{dz'}{E(z', \Theta)}}{\int_0^{z_s} \frac{dz'}{E(z', \Theta)}}, \quad (9)$$

where  $\Theta$  represents the free parameters for each cosmological model,  $z_l$  is the redshift of the lens and  $z_s$  is the redshift of the source. Therefore, we can constrain cosmological parameters minimizing the chi-square function,

$$\chi_{SL}^2(\Theta) = \sum_{i=1}^{N_{SL}} \frac{\left[ D^{th}(z_l, z_s; \Theta) - D^{obs}(\theta_E, \sigma^2) \right]^2}{(\delta D^{obs})^2}, \quad (10)$$

---

<sup>4</sup> The 99 systems give a physical angular diameter distance in  $y$ -redshift, but not all of them give a physical result in  $z$ -redshift.

where  $\delta D^{\text{obs}}$  is the standard error propagation of the observational lens equation (8),  $N_{SL}$  accounts for the number of strong lensing systems under consideration and  $D^{th}$  is given by Eq. (9).

The posterior probability density function (PDF) of the free parameters  $\Theta$  for each model is estimated through a Markov chain Monte Carlo (MCMC) Bayesian statistical analysis. We use the Affine Invariant MCMC Ensemble sampler from the `emcee` Python module [47] with 1000 burn-in steps, 1000 walkers, and 5000 MCMC steps. We estimate the cosmological parameters considering the likelihood function

$$\mathcal{L}(\Theta) \propto e^{-\chi_{\text{SL}}^2(\Theta)}, \quad (11)$$

where  $\chi_{\text{SL}}^2(\Theta)$  is given by Eq. ((10)). We assess chain convergence using the Gelman-Rubin test introduced by Gelman et al. (1992). The priors for the cosmological parameters of each model are the following: in the  $\omega$ CDM scenario we adopt a flat prior on  $\omega \in (-4, 1)$  and a Gaussian prior on  $\Omega_{0m} = 0.3111 \pm 0.0056$  according to Planck measurements [2], in the hFRW model we assume a flat prior on  $\Omega_{0B} \in (0, 1)$  and  $\Omega_{0\lambda} \in (0, 1)$ , finally in the model  $f(R, T)$  we considered a flat prior on  $n \in (0, 3)$ . To estimate the best fit value for the cosmological parameters we perform six runs employing two distinct data sets, one for each model (excluding the DHOST model). The DHOST model is addressed in a different way; since there is no analytical expression for  $H(z)$  and for  $D^{th}$ , various families of curves are constructed by varying the parameters  $c_2$  and  $\beta$ . In the first case, we vary  $c_2$  in the range  $[0.8, 1.2]$  with increments  $\Delta c_2 = 0.02$ , while keeping the remaining parameters fixed as  $c_3 = 5, c_4 = 1, \beta = -5.3$ . In the second case,  $\beta$  is taken in the range  $[-6, -2]$  with steps of 0.5, and  $c_2 = 1, c_3 = 5, c_4 = 1$ . These choices are motivated by the results of [38]. These curves are subsequently fitted using Eq. (10), and ultimately, the set of values corresponding to the solution that minimizes the likelihood function is chosen as the best fit for this model.

## B. Direct estimation of cosmographic parameters

The theoretical counterpart displayed in Eq. (9) is highly dependent on the form of  $E(z)$ . However, we can avoid considerations of a specific model of gravity by using a parameterization of  $E(z)$ , such as the one obtained in the cosmographic scenario. A detailed analysis of this scenario in the context of SLS is presented in [13], and the bases are explained in Appendix A. By using this, we obtain expressions for the distances between objects just in terms of their redshift and of derivatives of the scale factor, or the so called cosmographic parameters. Thus, in cosmography, Eq. (9) is approximated as

$$\begin{aligned} D^{th}(z_l, z_s; \Theta) &= \frac{(1 + z_s)^{-1} [\Delta(z_s) - \Delta(z_l)]}{D(z_s)} \\ &\approx \left(1 - \frac{z_l}{z_s}\right) - \frac{(1 + q_0)(z_s - z_l)z_l}{2z_s} + \mathcal{O}[z^2], \end{aligned} \quad (12)$$

where  $\Delta(z_l), \Delta(z_s)$  are the transverse comoving distances to the lens and source, respectively (see [13, 48] for more details).

As shown in [13], the parametrization of the redshift known as  $y$ -redshift [49], given by  $y(z) = z(1 + z)^{-1}$ , provides better constraints on the cosmographic parameters when using SLS. Therefore, it is convenient to express the theoretical lens equation in terms of  $y$ :

$$\begin{aligned} D^{th}(y_l, y_s; \Theta) &= \frac{(1 - y_s) [\Delta(y_s) - \Delta(y_l)]}{D(y_s)} \\ &\approx \frac{y_s - y_l}{y_s - y_s y_l} - \frac{(1 + q_0)(y_s - y_l)y_l}{2(y_s(-1 + y_l))^2} + \mathcal{O}[y^2], \end{aligned} \quad (13)$$

where  $\Delta(y_l), \Delta(y_s)$  are the transverse comoving distances to the lens and source in  $y$ -redshift space,  $y_s = y(z_s)$  and  $y_l = y(z_l)$ . With these results, we can also constrain the cosmographic parameters using the previously defined chi-square function (10), where  $D^{th}$  is now given by Eq. (12) when we want to constrain the cosmographic parameters in  $z$ -redshift. For  $y$ -redshift the equation for chi-square is essentially the same, but replacing  $D^{th}(z_l, z_s; \Theta)$  with  $D^{th}(y_l, y_s; \Theta)$  given by Eq. (13) and performing the appropriate transformations of the data and errors. We carried out two tests in the  $y$ -redshift space to estimate cosmographic parameters (one for each data set) assuming the following flat priors:  $-0.95 < q_0 < -0.2$ ,  $0 < j_0 < 2.0$ ,  $-2.0 < s_0 < 7.0$  and  $-5.0 < l_0 < 10.0$ .

### C. Assessing the applicability of cosmography

From Eq. (10) we can obtain the best fit values for the cosmographic parameters according to **SLS**. These values can be regarded as purely observational, and we refer to them as *direct cosmographic parameters*. On the other hand, different sets of *indirect* values for the cosmographic parameters can be obtained through the best fits for the free parameters of each model. These indirect parameters are obtained as follows. From the definition of the cosmographic parameters, we have

$$\left. \frac{dH}{dz} \right|_{z=0} = H_0(1 + q_0), \quad (14)$$

$$\left. \frac{1}{2!} \frac{d^2 H}{dz^2} \right|_{z=0} = \frac{H_0}{2}(-q_0^2 + j_0), \quad (15)$$

$$\left. \frac{1}{3!} \frac{d^3 H}{dz^3} \right|_{z=0} = \frac{H_0}{6}(3q_0^2 + 3q_0^3 - 4q_0 j_0 - 3j_0 - s_0), \quad (16)$$

$$\begin{aligned} \left. \frac{1}{4!} \frac{d^4 H}{dz^4} \right|_{z=0} = & \frac{H_0}{24}(-12q_0^2 - 24q_0^3 - 15q_0^4 + 32q_0 j_0 \\ & + 25q_0^2 j_0 + 7q_0 s_0 + 12j_0 - 4j_0^2 + 8s_0 + l_0). \end{aligned} \quad (17)$$

These equations can be inverted to give  $q_0, j_0, s_0, l_0$  in terms of the derivatives of  $H$  evaluated at  $z = 0$ ,

$$q_0 = \frac{H'}{H_0} - 1, \quad (18)$$

$$j_0 = \frac{H''}{H_0} + \left( \frac{H'}{H_0} - 1 \right)^2, \quad (19)$$

$$\begin{aligned} s_0 = & \frac{H'''}{H_0} - 3 \left( \frac{H'}{H_0} - 1 \right)^2 - 3 \left( \frac{H'}{H_0} - 1 \right)^3 + \\ & 4 \left( \frac{H'}{H_0} - 1 \right) \left( \frac{H''}{H_0} + \left( \frac{H'}{H_0} - 1 \right)^2 \right) + 3 \left( \frac{H''}{H_0} + \left( \frac{H'}{H_0} - 1 \right)^2 \right), \end{aligned} \quad (20)$$

where, just in this case, the prime represents derivatives with respect to the redshift evaluated at  $z = 0$ . A similar but more cumbersome expression can be obtained for  $l_0$ . For each model, these derivatives can be evaluated from Eqs. (1), (3), (5) and from the numerical solution for  $H$  in the case of DHOST, using the cosmological parameters adjusted through SLS. If cosmography provides a good representation of a model, we expect the direct and indirect values to be in agreement. As we show in the next section, this agreement is reached within  $2\sigma$  for all the models considered in this work (using the restricted sample).

Finally, we study the possibility of reconstructing the parameters of the models from the cosmographic parameters. To do so, we rewrite Eqs. (14)-(17) expressing the left hand sides with the corresponding expressions for each model, thus forming a systems of equations that can be solved for the parameters of the model in terms of the cosmographic parameters. Plugging in the direct values of the cosmographic parameters we obtain indirect estimations for the parameters of each model, which are then compared to their direct values obtained from Eq. (10). Once again, we find agreement within  $2\sigma$  when using the restricted SLS sample. This methodology can be useful for constraining parameters of modified gravity without performing a direct comparison with the observational data.

## IV. RESULTS

### A. Cosmological constraints

The best fit values for the density parameters of each model are shown in the bottom panels of Tables I and II for the restricted and fiduciary samples respectively. Additionally, we present the values of the indirect cosmographic parameters corresponding to each model through equations (14), (15), (16), and (17). For the cosmological constraints we find similar values with both samples, which are consistent at  $1\sigma$  in all cases. In the  $\omega$ CDM model (see Figure 2 to visualize the confidence contours and PDF) the value for  $\omega$  that we find is within  $1\sigma$  of the value reported by Planck ( $\omega = -1.56_{-0.48}^{+0.60}$ ) [2]; however, it is only consistent at  $2\sigma$  with a cosmological constant. It is noteworthy that



the value of  $\omega$  suggests the existence of a phantom dark energy in both cases. For the model hFRW (see Figure 3 to visualize confidence contours and PDF) both samples lead to values of  $\Omega_{0B}$  that are consistent at  $1\sigma$  with those obtained in [36] using supernova measurements, indicating lower values for  $\Omega_{0B} \sim 6\%$  than those of the  $\Lambda$ CDM model ( $\Omega_{0m} \sim 30\%$ ) where the inclusion of dark matter is required. On the other hand,  $\Omega_{0\lambda}$  is consistent with [36] at  $2\sigma$ . In the  $f(R, T)$  scenario (see figure 4) we obtain  $n = 1.033 \pm 0.05$  and  $n = 1.025 \pm 0.04$  for the restricted and fiduciary samples respectively, being consistent with a universe undergoing accelerated expansion as indicated in [41]. Finally, for the DHOST model arising from a numerical approximation, we obtain  $c_2 = 1.10$  and  $c_2 = 1.08$  for the restricted and fiduciary samples, respectively, slightly greater than a canonical kinetic term ( $c_2 = 1$ )<sup>5</sup>. The error is taken as 0.02, which was the variation of the parameter  $c_2$  among the different curves shown in Figure 1.

Param.	hFRW	$\omega$ CDM	$f(R, T)$	DHOST	Cosmo Obs.
$q_0$	$-0.84 \pm 0.06$	$-1.7 \pm 0.8$	$-0.484 \pm 0.025$	$-0.722 \pm 0.009$	$-0.54 \pm 0.1$
$j_0$	$1.0 \pm 1.3$	$8 \pm 7$	$0.25 \pm 0.08$	$0.475 \pm 0.027$	$0.36 \pm 0.52$
$s_0$	$0.0 \pm 692$	$37 \pm 79$	$0.1 \pm 0.4$	$1.42 \pm 0.24$	$3.7 \pm 3.31$
$l_0$	$0.0 \pm 5000$	$-600 \pm 1600$	$-0.6 \pm 3.1$	-	$-0.35 \pm 2.22$
Free Param	$\Omega_{0B} = 0.068 \pm 0.025$ $\Omega_{0\lambda} = 0.883 \pm 0.027$	$\Omega_{0m} = 0.31 \pm 0.005$ $\omega = -2.134 \pm 0.52$	$n = 1.033 \pm 0.05$	$c_2 = 1.10 \pm 0.02$	

TABLE I. Values for the cosmographic parameters obtained for each of the models of MG analyzed in the present work (upper panel). The values in the bottom panel are the density parameters obtained from the SLS data for each of the models through Bayesian statistical analysis. For both cases, here we used the sample of 99 SLS. The DHOST data are only computed up to the third parameter, as the numerical approximation lacks sufficient precision to obtain a solution up to fourth order.

Param.	hFRW	$\omega$ CDM	$f(R, T)$	DHOST	Cosmo Obs.
$q_0$	$-0.83 \pm 0.05$	$-1.2 \pm 0.5$	$-0.488 \pm 0.02$	$-0.713 \pm 0.01$	$-0.51 \pm 0.06$
$j_0$	$1.0 \pm 0.9$	$4.3 \pm 3.5$	$0.25 \pm 0.06$	$0.462 \pm 0.031$	$0.16 \pm 0.24$
$s_0$	$0.0 \pm 418$	$12 \pm 32$	$0.11 \pm 0.29$	$1.5 \pm 0.16$	$4.69 \pm 2.5$
$l_0$	$0.0 \pm 3200$	$-147 \pm 464$	$-0.6 \pm 3.1$	-	$-0.37 \pm 0.45$
Free Param	$\Omega_{0B} = 0.054 \pm 0.02$ $\Omega_{0\lambda} = 0.886 \pm 0.02$	$\Omega_{0m} = 0.308 \pm 0.006$ $\omega = -1.653 \pm 0.322$	$n = 1.025 \pm 0.04$	$c_2 = 1.08 \pm 0.02$	

TABLE II. Values for the cosmographic parameters obtained for each of the models of MG analyzed in the present work (upper panel). The values in the bottom are the density parameters predicted from the SLS data for each of the models. For both cases, we used here the sample of 143 SLS. The DHOST data are only computed up to the third parameter, as the numerical approximation lacks sufficient precision to obtain a solution up to fourth order.

## B. Contrast with cosmography

In the top panels of Tables I (99 SLS) and II (143 SLS) we show the indirect cosmographic parameters associated to each model. In addition, in the last column of each table we show the direct cosmographic parameters obtained in the  $y$ -redshift space for both data sets (similar values are reported in [13]). If we compare the values of the cosmographic parameters of each model at the present time with those arising directly from SLS measurements using cosmography, we can see that the  $q_0$  value is consistent at  $1\sigma$  only for the value given by the  $f(R, T)$  model, the remaining models are only consistent at  $2\sigma$  of the confidence level, excluding the DHOST and hFRW models for the fiduciary sample, which only exhibits consistency at  $3\sigma$ . It is worth noticing that all models are compatible with accelerated expansion. Regarding the parameter  $j_0$ , most of the models are in agreement at  $1\sigma$  of the confidence level with the one obtained directly from cosmography, except for the  $\omega$ CDM model and the DHOST model analysed with the fiduciary sample, which are consistent at  $2\sigma$ . For the remaining two parameters  $s_0$  and  $l_0$ , the majority are consistent at  $1\sigma$  of confidence level with those obtained directly from cosmography, except for models  $f(R, T)$

<sup>5</sup> Although  $c_2$  can be absorbed in a redefinition of the scalar field, this would modify the other coupling constants.

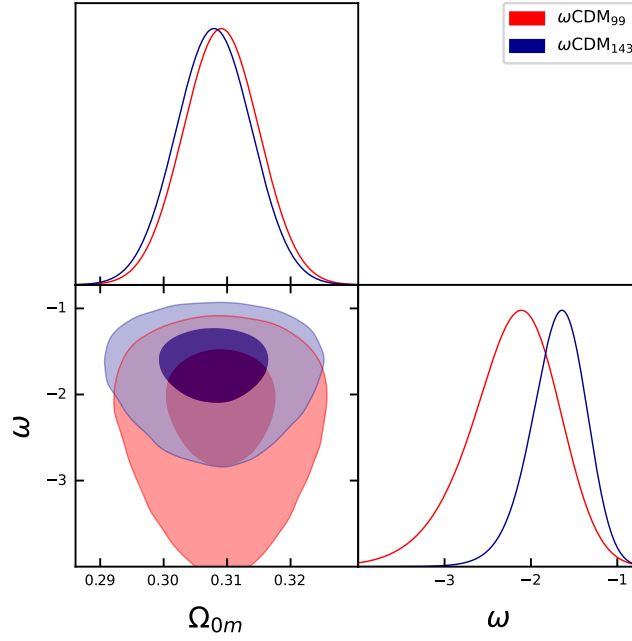


FIG. 2. 1D marginalized posterior distributions and the 2D 68%, 99.7% confidence levels for the  $\Omega_{m0}$  and  $\omega$  parameters for the  $\omega$ CDM model using a restricted sample of 99 SLS (red) and a sample of 143 SLS (dark blue).

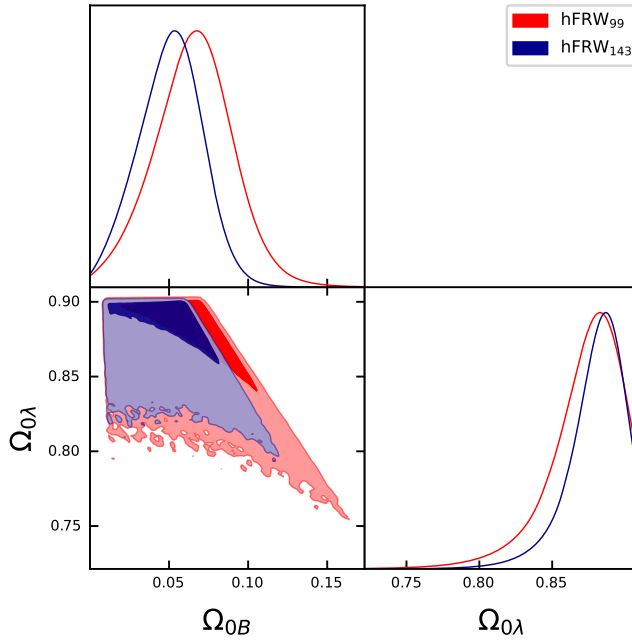


FIG. 3. 1D marginalized posterior distributions and the 2D 68%, 99.7% confidence levels for the  $\Omega_b$  and  $\Omega_\lambda$  parameters for the hFRW model using a restricted sample of 99 SLS (red) and a sample of 143 SLS (dark blue).

and DHOST (using the fiduciary sample), which demonstrate consistency up to  $2\sigma$ . Furthermore, it is observed that the errors in the cosmographic parameters tend to increase as more orders of expansion are considered. This growth pattern aligns with the observations reported in studies using SN Ia data, as exemplified by [11].

In order to get some insight into the meaning of the values presented above, we take the comparison to the level of the Hubble factor. For each model, we construct an *indirect cosmographic Hubble factor* by evaluating Eq. (A12) with the corresponding indirect cosmographic parameters. In Fig. 5, we compare these indirect Hubble factors to



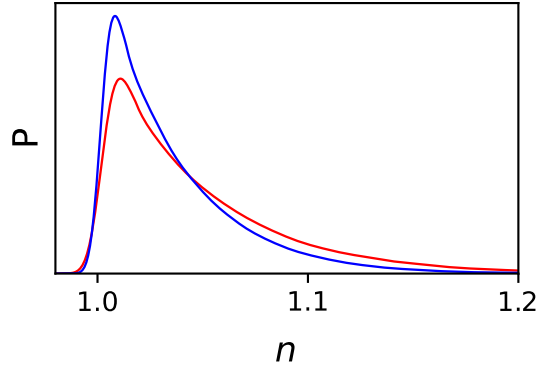


FIG. 4. 1D marginalized posterior distributions for the  $n$  parameter on the  $f(R, T)$  model for a restricted sample of 99 SLS (red) and a sample of 143 SLS (blue).

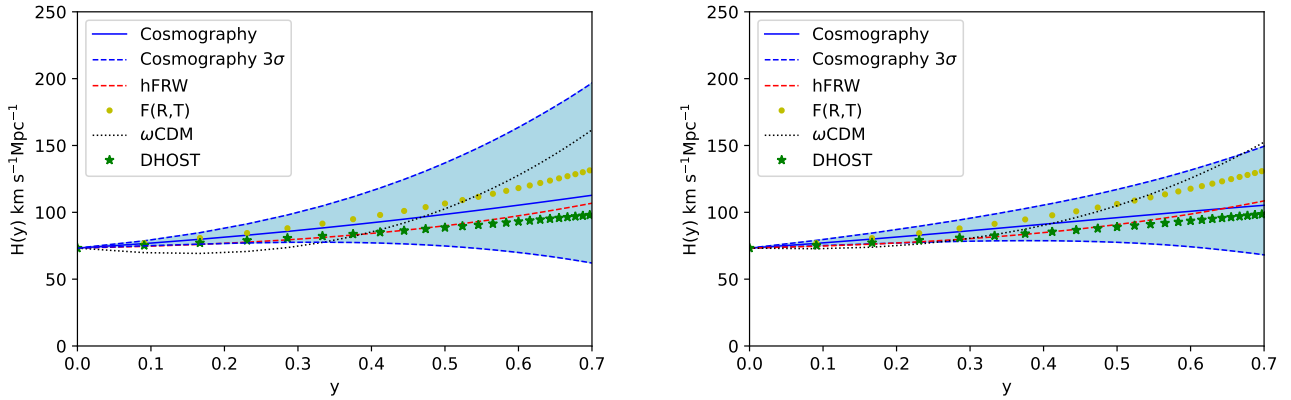


FIG. 5. Comparison of the  $H(y)$  function in terms of the cosmographic parameters for each model and the one obtained from cosmography directly with 99 (left) and 143 (right) SLS.

the one obtained with the direct cosmographic parameters. We also show the  $3\sigma$  confidence region of the direct Hubble factor, obtained by propagating the Markov chains of the statistical analysis. As a quantitative measure of the difference between direct and indirect Hubble factors, we use the mean relative error. We found similar results for both samples, with the hFRW model showing the minimum deviation from the true model, obtaining 6.7% and 3.6% for restricted and fiduciary samples, respectively. The second model with the smallest difference was the DHOST model, which produced a disparity of 9.5% for the restricted sample and 6% for the fiduciary sample. Subsequently, the model  $f(R, T)$  secured the third position, showing a discrepancy of 9.6% and 13.2%, respectively. Finally, the model with a larger scatter was  $\omega$ CDM, which yielded a relative error of approximately 20% for both data sets. Since each cosmological model has a different number of free parameters, in the following section, we present an analysis that takes this into consideration.

### C. Model selection

As a final test of the compatibility between cosmography and the models of modified gravity under consideration, we use model selection criteria. Specifically, we investigate whether these criteria give consistent results when applied either to the models fitted directly with SLS or to their indirect cosmographic approximations. Model selection aims to strike a balance between the accuracy of fitting observational data and the predictiveness of the model that achieves such a fit. This balance is attained through a criterion that assigns a numerical value to each model, enabling the creation of a rank-ordered list. We employ the Bayesian information criterion [BIC, 50] and the Akaike information

criterion [AIC, 51]. These criteria are defined by

$$\text{BIC} = \chi_{min}^2 + k \ln N, \quad (21)$$

$$\text{AIC} = \chi_{min}^2 + 2k, \quad (22)$$

where  $N$  stands for the number of data points,  $k$  is the number of parameters and  $\chi_{min}^2$  is the chi-square function. When these criteria are applied to the models fitted directly with SLS,  $\chi_{min}^2$  is evaluated with the best fit cosmological values from the bottom panels of tables I and II. On the other hand, when the criteria are applied to the cosmographic approximations,  $\chi_{min}^2$  is evaluated using the theoretical lens equation (13) expressed in terms of the cosmographic parameters in  $y$ -redshift space, and taking the indirect cosmographic parameters from the corresponding columns of tables I and II. Tables III and IV show the values of the selection criteria for both approaches. Furthermore, we present the reduced chi-square  $\chi_{red}^2 = \chi_{min}^2 / (N - k)$  and the  $\Delta\text{BIC} = \text{BIC}_i - \text{BIC}_{min}$  ( $\Delta\text{AIC} = \text{AIC}_i - \text{AIC}_{min}$ ), which is a relative value of BIC (AIC) for model  $i$  compared to the minimum  $\text{AIC}_{min}$  ( $\text{BIC}_{min}$ ) among all models (see [52] for details). Considering the current datasets, the hFRW model is favored by all model selection tests; however, for the sample of 99 SLS, the preferred model (in the cosmographic approach) is the DHOST model; nevertheless, the values for  $\Delta\text{BIC}$ ,  $\Delta\text{AIC}$ , and  $\chi_{red}^2$  are very close to those obtained for the hFRW model, showing not enough evidence to discern between both models. Furthermore, the least accepted model was the  $\omega\text{CDM}$  model. This could be due to the Gaussian prior (from Planck measurements) on  $\Omega_{0m}$ , which appears to impact the model's compatibility with SLS. Assuming such a prior is necessary due to the inability to properly constrain the value of  $\Omega_{0m}$  with SLS at galactic scales [17, 53]. It is worth noticing that departures from  $\Lambda\text{CDM}$  using measurements at galaxy cluster scales have been previously found in [22, 54], and more recently, employing observations from both scales in [30].

Model	Free parameters	$\chi_{SLS}^2$	$\chi_{red}^2$	AIC	BIC	$\Delta\text{AIC}$	$\Delta\text{BIC}$
<i>hFRW</i>	2	177.624	1.831	181.624	187.550	0	0
$\omega\text{CDM}$	2	192.773	1.987	196.773	201.963	15.149	14.413
$f(R, T)$	1	190.978	1.948	192.978	195.573	11.354	8.023
DHOST	1	190.326	1.942	192.326	194.921	10.702	7.371
<i>hFRW<sub>C</sub></i>	2	121.255	1.250	125.255	130.445	1.104	3.699
$\omega\text{CDM}_C$	2	620.986	6.40	624.986	630.176	500.835	503.436
$f(R, T)_C$	1	132.845	1.355	134.845	137.440	10.334	10.694
DHOST <sub>C</sub>	1	122.151	1.246	124.151	126.746	0	0

TABLE III. Model selection criteria for the restricted sample with a total of 99 SLS. The subscript C indicates that the chi-square function (10) was constructed using the cosmography parameters to a third-order approximation of each cosmological model and extracted from table I.

Model	Free parameters	$\chi_{SLS}^2$	$\chi_{red}^2$	AIC	BIC	$\Delta\text{AIC}$	$\Delta\text{BIC}$
<i>hFRW</i>	2	231.103	1.639	235.103	241.029	0	0
$\omega\text{CDM}$	2	263.795	1.871	267.795	273.721	32.692	32.692
$f(R, T)$	1	243.121	1.712	245.121	247.716	10.018	6.687
DHOST	1	253.170	1.783	255.170	258.133	20.067	17.104
<i>hFRW<sub>C</sub></i>	2	168.139	1.192	172.139	178.065	0	0
$\omega\text{CDM}_C$	2	436.528	3.096	440.528	446.453	268.389	268.388
$f(R, T)_C$	1	193.435	1.362	195.435	198.398	23.296	20.333
DHOST <sub>C</sub>	1	179.782	1.266	183.782	184.745	11.643	6.68

TABLE IV. Model selection criteria for the fiduciary sample with a total of 143 SLS. The subscript C indicates that the chi-square function 10 was constructed through the cosmography parameters to a third-order approximation of each cosmological model extracted from table II.

Model	99 SLS	143 SLS
$f(R, T)$	$n = 0.92 \pm 0.2$	$n = 0.98 \pm 0.12$
$\omega$ CDM	$\Omega_{0m} = 0.13 \pm 0.23$	$\Omega_{0m} = 0.07 \pm 0.13$
	$\omega_0 = -0.77 \pm 0.21$	$\omega_0 = -0.72 \pm 0.11$
hFRW	$\Omega_{0B} = 0.37 \pm 0.26$	$\Omega_{0B} = 0.42 \pm 0.12$
	$\Omega_{0\lambda} = 0.59 \pm 0.28$	$\Omega_{0\lambda} = 0.55 \pm 0.13$
DHOST	$c_2 = 0.82 \pm 0.12$	$c_2 = 0.78 \pm 0.10$

TABLE V. The values presented here are the values for the density parameters of each cosmological model computed directly from the cosmographic parameters obtained from direct observations of the SLS data. Errors are calculated at  $1\sigma$  of the confidence level.

#### D. Reconstruction

So far we have verified in detail the compatibility between cosmography and some models of modified gravity emerging from diverse theoretical scenarios. This supports the idea that one should be able to predict the best fit for the cosmological parameters of MG models using cosmography, i.e. without the need of a direct fit between the models and observational data. This is what we explore in this section. We reverse the procedure from equations (14-17), now using the cosmographic parameters obtained directly from SLS to compute the density parameters of each model (see table V). These values are to be compared with the direct fits provided in Tables I and II. In the  $\omega$ CDM scenario, we find a discrepancy beyond  $2\sigma$  in the estimation of  $\omega$  when using the sample with 143 SLS. Similar results are obtained for the other models, although with smaller uncertainties. Figures 6 and 7 illustrate the comparison between direct and indirect values of the cosmological parameters. For the reduced sample of 99 SLS, all the parameters are compatible at  $2\sigma$ . Therefore, we recommend the use of the restricted sample for estimating cosmological parameters.

As the previous discussion shows, the reverse procedure gives a reasonable estimation of the parameters of each model. Nevertheless, we see two issues:

**Error propagation:** The complexity of the algebraic expressions resulting from solving (14-17) for the parameters of the model leads to large uncertainties due to error propagation. This can be reduced by improving the error bars of the cosmographic parameters with the inclusion of more data sets.

**Over-determined system:** While there is an arbitrary number of cosmographic parameters (depending on the order of approximation), there is only a finite and fixed number of parameters of each model. Therefore, the process is over-determined, since only a subset of equations (14-17) needs to be used, allowing for different values to be obtained in the estimation of the density parameters. We suggest employing the necessary equations in ascending order since lower-order terms are more relevant in cosmography, and also to avoid even larger error propagation – lowest order expressions are usually simpler.

Summarising, it is possible to use the reverse process described here in order to get a quick estimation of the parameters of a MG model, but it is essential to take into account the uncertainties of the cosmographic parameters and the resulting error propagation, and to interpret the results as a range where the model is compatible with the set of observations used to derive the cosmographic parameters.

#### V. DISCUSSION

The main objective of this work was to analyze a methodology that allows for a simple and fast comparison between predictions of modified gravity and direct results from observations. The simplicity of this methodology relies on the fact that one does not need to evaluate the observables in the modified theory of gravity; instead, one only needs a numerical or analytic expression for the Hubble parameter of the theory. With this expression at hand, one can find a relation between the parameters of the theory and a kinematical parameterization of the properties of the universe, called cosmography.

In order to assess the validity of this methodology, we use a two-step process. First, we obtain the best fit parameters of the model, taking into consideration strong lensing observations in which an elliptical galaxy acts as a lens. With these parameters, we estimate indirect values for the cosmographic parameters and compare them to the direct best fits for cosmography obtained with the same data set. This step gives us information on the compatibility between the models and cosmography. In most cases we find good agreement within  $2\sigma$  of confidence level. As a complement

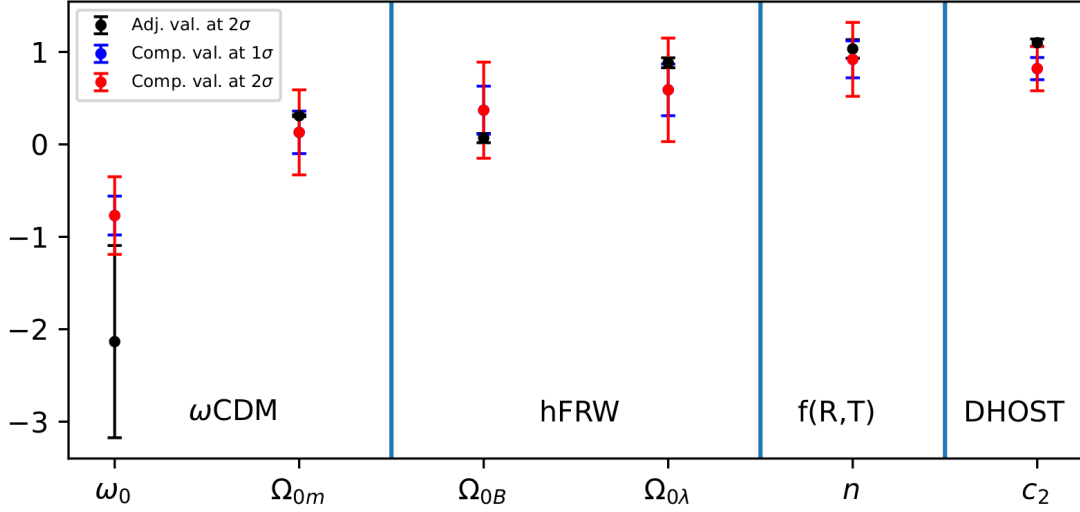


FIG. 6. Density parameters of each cosmological model computed in terms of the direct cosmographic parameters obtained from the restricted sample of 99 SLS (see upper-right column of table I). These parameters were computed using the process described in section III C. The black color indicates the value of the adjustment with observational data, and the blue and red colors indicate the value computed from the cosmographic parameters adjusted from observations at  $1\sigma$  and  $2\sigma$  respectively

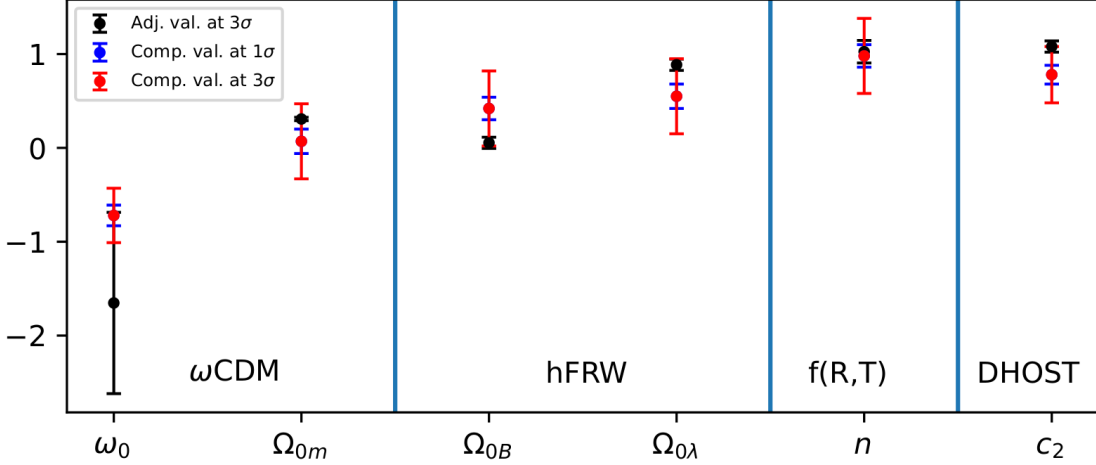


FIG. 7. Density parameters of each cosmological model computed in terms of the direct cosmographic parameters obtained from the fiduciary sample of 143 SLS (see upper-right column of table II). These parameters were computed using the process described in section III C. The black color indicates the value of the adjustment with observational data, and the blue and red colors indicate the value computed from the cosmographic parameters adjusted from observations at  $1\sigma$  and  $3\sigma$  respectively

to this step, we compare the 3th order cosmographic expressions for  $H(y)$  evaluated with the direct and indirect cosmographic parameters. The smallest mean relative difference was for hFRW, showing a value less than 7% for both data sets. As a further analysis in this first step, we subjected the models to different statistical selection tests. The results of these tests are consistent with each other, indicating that the preferred model was hFRW. This result should be taken with caution, as the true model should be favored by all astrophysical observations; therefore, it is necessary to subject this model to more sets of observational data.

Now, the second step is to determine quantitatively whether cosmography can be used to reconstruct the best fit parameters of each model. From a mathematical point of view, this is not straightforward, since the system of equations may be over-determined. For example, if a model contains only one parameter, then Eqs. (14-17) can be manipulated to obtain 4 different equations for the parameters given in terms of given values of  $q_0, j_0, s_0$  and  $l_0$ . Since in cosmography these values are independent, the four equations lead, in principle, to four different values for the only parameter of the model. The reasonable choice then is to start from the lowest orders and solve until we obtain values

for all the parameters of the model. In this way, we find that the parameters of the model can indeed be reconstructed within  $2\sigma$  of confidence level.

It is important to note that this work was conducted assuming a Maclaurin series, i.e., around  $z = 0$  ( $y = 0$ ) which corresponds to the present day of the Universe. Therefore, the accuracy decreases away from that point, as can be observed in Fig. 5. Alternatively, the expansion could be around another point to obtain accurate information about different stages of the Universe, for example, at the transition redshift or even in the early Universe. This underscores the necessity of exploring, in future research, different approaches to cosmography and diverse astrophysical observations at different epochs in the Universe, which can lead to more robust and stronger constraints.

In conclusion, this study underscores the importance of investigating the relations among various cosmological models and cosmography. Understanding these relationships yields practical applications to modified gravity scenarios – even if the solutions are known only numerically – such as the possibility to probe the validity of MG with observational data in an efficient manner.

## ACKNOWLEDGMENTS

AL is supported by CONAHCyT-855158. MHA acknowledges support from *Estancias Posdoctorales CONAHCyT*. JC is partially supported by DCF-320821.

## REFERENCES

- 
- [1] Adam G. Riess, Alexei V. Filippenko, Peter Challis, Alejandro Clocchiatti, Alan Diercks, et al. Observational evidence from supernovae for an accelerating universe and a cosmological constant. *The Astronomical Journal*, 116(3):1009, 1998.
  - [2] N. Aghanim et al. Planck 2018 results. VI. Cosmological parameters. *Astron. Astrophys.*, 641:A6, 2020. [Erratum: *Astron. Astrophys.* 652, C4 (2021)].
  - [3] Graeme E. Addison, Gary Hinshaw, and Mark Halpern. Cosmological constraints from baryon acoustic oscillations and clustering of large-scale structure. *Mon. Not. Roy. Astron. Soc.*, 436:1674–1683, 2013.
  - [4] Seshadri Nadathur, Will J. Percival, Florian Beutler, and Hans Winther. Testing Low-Redshift Cosmic Acceleration with Large-Scale Structure. *Phys. Rev. Lett.*, 124(22):221301, 2020.
  - [5] Elcio Abdalla et al. Cosmology intertwined: A review of the particle physics, astrophysics, and cosmology associated with the cosmological tensions and anomalies. *JHEAp*, 34:49–211, 2022.
  - [6] Eleonora Di Valentino, Olga Mena, Supriya Pan, Luca Visinelli, Weiqiang Yang, Alessandro Melchiorri, David F. Mota, Adam G. Riess, and Joseph Silk. In the realm of the Hubble tension—a review of solutions. *Class. Quant. Grav.*, 38(15):153001, 2021.
  - [7] Tsutomu Kobayashi, Masahide Yamaguchi, and Jun’ichi Yokoyama. Generalized G-inflation: Inflation with the most general second-order field equations. *Prog. Theor. Phys.*, 126:511–529, 2011.
  - [8] Philippe Brax. Screening mechanisms in modified gravity. *Class. Quant. Grav.*, 30:214005, 2013.
  - [9] Austin Joyce, Bhuvnesh Jain, Justin Khoury, and Mark Trodden. Beyond the Cosmological Standard Model. *Phys. Rept.*, 568:1–98, 2015.
  - [10] Vinicius C. Busti, Alvaro de la Cruz-Dombriz, Peter K. S. Dunsby, and Diego Saez-Gomez. Is cosmography a useful tool for testing cosmology? *Phys. Rev.*, D92(12):123512, 2015.
  - [11] Ming-Jian Zhang, Hong Li, and Jun-Qing Xia. What do we know about cosmography. *The European Physical Journal C*, 77(7), jun 2017.
  - [12] Giada Bargiacchi, G. Risaliti, M. Benetti, S. Capozziello, E. Lusso, A. Saccardi, and M. Signorini. Cosmography by orthogonalized logarithmic polynomials. *Astron. Astrophys.*, 649:A65, 2021.
  - [13] Andrés Lizardo, Mario H. Amante, Miguel A. García-Aspeitia, Juan Magaña, and V. Motta. Cosmography using strong-lensing systems and cosmic chronometers. *Mon. Not. Roy. Astron. Soc.*, 507(4):5720–5731, 2021.
  - [14] Juan Magaña, Mario H. Amante, Miguel A. García-Aspeitia, and V. Motta. The Cardassian expansion revisited: constraints from updated Hubble parameter measurements and type Ia supernova data. *Mon. Not. Roy. Astron. Soc.*, 476(1):1036–1049, 2018.
  - [15] Jéferson A. S. Fortunato, Wiliam S. Hipólito-Ricaldi, and Marcelo V. dos Santos. Cosmography from well-localized Fast Radio Bursts. 7 2023.
  - [16] G. Bargiacchi, M. G. Dainotti, and S. Capozziello. Tensions with the flat  $\Lambda$ CDM model from high-redshift cosmography. 7 2023.
  - [17] Mario H. Amante, Juan Magaña, V. Motta, Miguel A. García-Aspeitia, and Tomás Verdugo. Testing dark energy models with a new sample of strong-lensing systems. *Mon. Not. Roy. Astron. Soc.*, 498(4):6013–6033, 2020.

- [18] C. Grillo, M. Lombardi, and G. Bertin. Cosmological parameters from strong gravitational lensing and stellar dynamics in elliptical galaxies. *Astron. Astrophys.*, 477:397, 2008.
- [19] Eric Jullo, Priyamvada Natarajan, Jean-Paul Kneib, Anson D’Aloisio, Marceau Limousin, Johan Richard, and Carlo Schmid. Cosmological Constraints from Strong Gravitational Lensing in Galaxy Clusters. *Science*, 329:924–927, 2010.
- [20] Juan Magaña, V. Motta, Victor H. Cardenas, T. Verdugo, and Eric Jullo. A magnified glance into the dark sector: probing cosmological models with strong lensing in A1689. *Astrophys. J.*, 813(1):69, 2015.
- [21] Juan Magana, Ana Acebron, Veronica Motta, Tomas Verdugo, Eric Jullo, and Marceau Limousin. Strong lensing modeling in galaxy clusters as a promising method to test cosmography I. Parametric dark energy models. *Astrophys. J.*, 865(2):122, 2018.
- [22] G. B. Caminha, S. H. Suyu, C. Grillo, and P. Rosati. Galaxy cluster strong lensing cosmography - Cosmological constraints from a sample of regular galaxy clusters. *Astron. Astrophys.*, 657:A83, 2022.
- [23] Alessandro Sonnenfeld. Statistical strong lensing - II. Cosmology and galaxy structure with time-delay lenses. *Astron. Astrophys.*, 656:A153, 2021.
- [24] Michele Moresco et al. Unveiling the Universe with emerging cosmological probes. *Living Rev. Rel.*, 25(1):6, 2022.
- [25] Peng-Ju Wu, Yue Shao, Shang-Jie Jin, and Xin Zhang. A path to precision cosmology: synergy between four promising late-universe cosmological probes. *JCAP*, 06:052, 2023.
- [26] Jing-Wang Diao, Yu Pan, and Wenxiao Xu. Testing the Coincidence Problem with Strong Gravitational Lens, Type Ia Supernovae and Hubble Parameter Observational Data. *Res. Astron. Astrophys.*, 22(11):115019, 2022.
- [27] Jing-Zhao Qi, Wei-Hong Hu, Yu Cui, Jing-Fei Zhang, and Xin Zhang. Cosmological Parameter Estimation Using Current and Future Observations of Strong Gravitational Lensing. *Universe*, 8(5):254, 2022.
- [28] S. Birrer, M. Millon, D. Sluse, A. J. Shajib, F. Courbin, L. V. E. Koopmans, S. H. Suyu, and T. Treu. Time-Delay Cosmography: Measuring the Hubble Constant and other cosmological parameters with strong gravitational lensing. 10 2022.
- [29] Tommaso Treu, Sherry H. Suyu, and Philip J. Marshall. Strong lensing time-delay cosmography in the 2020s. *Astron. Astrophys. Rev.*, 30(1):8, 2022.
- [30] Tomás Verdugo, Mario H. Amante, Juan Magaña, Miguel A. García-Aspeitia, Alberto Hernández-Almada, and Verónica Motta. Synchronize your \textit{titchrono}-brane: Testing a variable brane tension model with strong gravitational lensing. 1 2024.
- [31] Masashi Chiba. Probing dark matter substructure in lens galaxies. *Astrophys. J.*, 565:17, 2002.
- [32] Henk Hoekstra, Howard K. C. Yee, and Michael D. Gladders. Properties of galaxy dark matter halos from weak lensing. *Astrophys. J.*, 606:67–77, 2004.
- [33] Richard Massey, Thomas Kitching, and Johan Richard. The dark matter of gravitational lensing. *Rept. Prog. Phys.*, 73:086901, 2010.
- [34] Nick Kaiser and Gordon Squires. Mapping the dark matter with weak gravitational lensing. *Astrophys. J.*, 404:441–450, 1993.
- [35] Rong-Gen Cai, Sichun Sun, and Yun-Long Zhang. Emergent Dark Matter in Late Time Universe on Holographic Screen. *JHEP*, 10:009, 2018.
- [36] Rong-Gen Cai, Sunly Khimphun, Bum-Hoon Lee, Sichun Sun, Gansukh Tumurtushaa, and Yun-Long Zhang. Emergent Dark Universe and the Swampland Criteria. *Phys. Dark Univ.*, 26:100387, 2019.
- [37] Javier Chagoya, I. Díaz-Saldaña, J. C. López-Domínguez, and M. Sabido. Cosmic acceleration in entropic cosmology. 5 2023.
- [38] Marco Crisostomi and Kazuya Koyama. Self-accelerating universe in scalar-tensor theories after GW170817. *Phys. Rev. D*, 97(8):084004, 2018.
- [39] Adam G. Riess et al. A 2.4% Determination of the Local Value of the Hubble Constant. *Astrophys. J.*, 826(1):56, 2016.
- [40] Adam G. Riess et al. A Comprehensive Measurement of the Local Value of the Hubble Constant with  $1 \text{ km s}^{-1} \text{ Mpc}^{-1}$  Uncertainty from the Hubble Space Telescope and the SH0ES Team. *Astrophys. J. Lett.*, 934(1):L7, 2022.
- [41] Ritika Nagpal, S. K. J. Pacif, J. K. Singh, Kazuharu Bamba, and A. Beesham. Analysis with observational constraints in  $\Lambda$ -cosmology in  $f(R, T)$  gravity. *Eur. Phys. J. C*, 78(11):946, 2018.
- [42] Peter Schneider. *Extragalactic Astronomy and Cosmology*. 2006.
- [43] Christopher S. Kochanek. Evidence for Dark Matter in MG 1654+134. *Astrophys. J.*, 445:559, June 1995.
- [44] Tommaso Treu and Leon Koopmans. The internal structure and formation of early-type galaxies: the gravitational-lens system mg2016+112 at  $z=1.004$ . *Astrophys. J.*, 575:87, 2002.
- [45] L. V. E. Koopmans and T. Treu. The structure and dynamics of luminous and dark matter in the early-type lens galaxy of 0047-281 at  $z=0.485$ . *Astrophys. J.*, 583:606–615, 2003.
- [46] D. Rusin, C. S. Kochanek, and C. R. Keeton. Selfsimilar models for the mass profiles of early-type lens galaxies. *Astrophys. J.*, 595:29–42, 2003.
- [47] Daniel Foreman-Mackey, David W. Hogg, Dustin Lang, and Jonathan Goodman. emcee: The MCMC Hammer. *Publications of the Astronomical Society of the Pacific*, 125(925):306, March 2013.
- [48] David W. Hogg. Distance measures in cosmology. 5 1999.
- [49] Céline Cattoën and Matt Visser. The hubble series: convergence properties and redshift variables. *Classical and Quantum Gravity*, 24(23):5985–5997, November 2007.
- [50] Gideon Schwarz. Estimating the Dimension of a Model. *Annals Statist.*, 6:461–464, 1978.
- [51] H. Akaike. A new look at the statistical model identification. *IEEE Trans. Automatic Control*, 19(6):716–723, 1974.

- [52] Ke Shi, Yongfeng Huang, and Tan Lu. A comprehensive comparison of cosmological models from latest observational data. *Mon. Not. Roy. Astron. Soc.*, 426:2452–2462, 2012.
- [53] Yun Chen, Ran Li, Yiping Shu, and Xiaoyue Cao. Assessing the effect of lens mass model in cosmological application with updated galaxy-scale strong gravitational lensing sample. *Mon. Not. Roy. Astron. Soc.*, 488(3):3745–3758, 2019.
- [54] Marceau Limousin, Benjamin Beauchesne, and Eric Jullo. Dark matter in galaxy clusters: Parametric strong-lensing approach. *Astron. Astrophys.*, 664:A90, 2022.

### Appendix A: Cosmography in the $y$ -redshift scenario

The foundations of this work are placed in a technique known as cosmography, this is purely the study of the kinematics of the Universe by the determination of parameters defined as quantities related to the derivatives of the scale factor. For a detailed formulation we start with the scale factor  $a(t)$  and expand it as a Taylor series around  $t = t_0$

$$a(t) = a(t_0) + \dot{a}(t_0)(t - t_0) - \frac{1}{2}\ddot{a}(t_0)(t - t_0)^2 + \dots, \quad (\text{A1})$$

and from here we divide the expression by  $a(t_0)$  in order to obtain

$$\frac{a(t)}{a(t_0)} = 1 + H_0(t - t_0) - \frac{q_0}{2}H_0^2(t - t_0)^2 + \dots, \quad (\text{A2})$$

where

$$q_0 \equiv -\frac{\ddot{a}(t_0)a(t_0)}{\dot{a}(t_0)^2}, \quad (\text{A3})$$

is the so called *deceleration parameter*. As we can see, this parameter is dimensionless, and it is directly proportional to the second derivative of the scale factor. The suffix 0 stands for present time parameters. Similarly, we define parameters related to higher order derivatives, which are named *cosmographic parameters*,

$$q \equiv -\frac{1}{a} \frac{d^2 a}{dt^2} \left[ \frac{1}{a} \frac{da}{dt} \right]^2, \quad (\text{A4})$$

$$j \equiv \frac{1}{a} \frac{d^3 a}{dt^3} \left[ \frac{1}{a} \frac{da}{dt} \right]^3, \quad (\text{A5})$$

$$s \equiv \frac{1}{a} \frac{d^4 a}{dt^4} \left[ \frac{1}{a} \frac{da}{dt} \right]^4, \quad (\text{A6})$$

$$l \equiv \frac{1}{a} \frac{d^5 a}{dt^5} \left[ \frac{1}{a} \frac{da}{dt} \right]^5, \quad (\text{A7})$$

where  $j$  is known as  *jerk*,  $s$  is called  *snap* and  $l$  is named  *lerk parameter*. Then equation (A2) can be expressed as,

$$\frac{a(t)}{a(t_0)} = 1 + H_0(t - t_0) - \frac{1}{2}q_0 H_0^2(t - t_0)^2 + \frac{1}{6}j_0 H_0^3(t - t_0)^3 \quad (\text{A8})$$

$$+ \frac{1}{24}s_0 H_0^4(t - t_0)^4 + \frac{1}{120}l_0 H_0^5(t - t_0)^5 + \mathcal{O}(t^6). \quad (\text{A9})$$

With a similar procedure we expand the Hubble factor into a Taylor series in terms of the redshift, and by using the previous definitions of the cosmographic parameters (equations A4, A5, A6 and A7 ) we find an algebraic expression in the following way:

$$\begin{aligned} H(z) &= H_0 + \left. \frac{dH}{dz} \right|_{z=0} z + \frac{1}{2!} \left. \frac{d^2 H}{dz^2} \right|_{z=0} z^2 + \frac{1}{3!} \left. \frac{d^3 H}{dz^3} \right|_{z=0} z^3 + \dots \\ &= H_0 \left[ 1 + (1 + q_0)z + \frac{1}{2}(-q_0^2 + j_0)z^2 + \frac{1}{6}(3q_0^2 + 3q_0^3 - 4q_0 j_0 - 3j_0 - s_0)z^3 \right. \\ &\quad \left. + \frac{1}{24}(-12q_0^2 - 24q_0^3 - 15q_0^4 + 32q_0 j_0 + 25q_0^2 j_0 + 7q_0 s_0 + 12j_0 - 4j_0^2 + 8s_0 + l_0)z^4 \right. \\ &\quad \left. + \mathcal{O}(z^5) \right]. \end{aligned} \quad (\text{A10})$$



Cosmographic parameter	Value obtained
$q_0$	$-0.313 \pm 0.018$
$j_0$	$1.83 \pm 0.045$
$s_0$	$2.207 \pm 0.4656$
$l_0$	$-0.5983 \pm 0.0544$

TABLE VI. Values for the cosmographic parameters up to 4th order in the  $z$ -redshift scenario, obtained with the set of 99 SLS data

We conduct an additional test (using the MCMC bayesian analysis) in the  $z$ -redshift for the restricted sample. The values of the cosmographic parameters are reported in Table VI. The aforementioned parametrization presents fitting difficulties in zones where the redshift  $z$  is away from the origin ( $z = 0$ ), in order to avoid this problem, we need a parameterization that can map the whole redshift spectrum into a closer region where the expansion is made (see [13] for details). Here, we employ the so-called  $y$ -redshift parametrization, first proposed by Celine Cattoen et. al. in [49], given as,

$$y = \frac{z}{1+z}, \quad (\text{A11})$$

expressing the analogous equation to A10 in terms of the  $y$ -redshift, we obtain

$$\begin{aligned} H(y) = & H_0 \left[ 1 + (1 + q_0)y + \frac{1}{2}(2 + 2q_0 - q_0^2 + j_0)y^2 \right. \\ & + \frac{1}{6}(6 + 6q_0 - 3q_0^2 + 3q_0^3 - 4q_0j_0 + 3j_0 - s_0)y^3 \\ & + \frac{1}{24}(24 - 4j_0^2 + l_0 + 24q_0 - 12q_0^2 + 12q_0^3 - 15q_0^4 \\ & + j_0(12 - 16q_0 + 25q_0^2) - 4s_0 + 7q_0s_0)y^4 \\ & \left. + \mathcal{O}(y^5) \right], \end{aligned} \quad (\text{A12})$$

which is the Hubble parameter in terms of the  $y$ -redshift, expanded as a taylor series around  $y = 0$ . An advantage of transitioning to the  $y$ -redshift space, is that it remains valid for higher values of the redshift. This is illustrated in Figure 8, where we compare the Friedmann equations in terms of cosmographic parameters obtained through  $z$ -redshift and  $y$ -redshift parametrizations (through an MCMC analysis), providing a better fit to the data from cosmic chronometers (presented in [14]) in the  $y$ -redshift space up to  $z \sim 1.3$ . Therefore, we have selected this parameterization because SLS encompasses higher redshifts than those presented in cosmic chronometers measurements.

## Appendix B: DHOST Lagrangians

Considering DHOST with up to quadratic terms in second order derivatives of the scalar field, the general Lagrangian has the form

$$\mathcal{L}_{quad} = G_2(X) + G_3(X)\Box\phi + \sum_{i=1}^5 \mathcal{L}_i + G(X)R + \mathcal{L}_m, \quad (\text{B1})$$

where  $X = \phi_\mu\phi^\mu$ ,  $R$  is the Ricci scalar of the metric  $g_{\mu\nu}$ ,  $\mathcal{L}_m$  is a Lagrangian for matter minimally coupled to the metric, and the Lagrangians  $\mathcal{L}_i$  are defined as

$$\mathcal{L}_1[A_1] = A_1(X)\phi_{\mu\nu}\phi^{\mu\nu}, \quad (\text{B2})$$

$$\mathcal{L}_2[A_2] = A_2(X)(\Box\phi)^2, \quad (\text{B3})$$

$$\mathcal{L}_3[A_3] = A_3(X)(\Box\phi)\phi^\mu\phi_{\mu\nu}\phi^\nu, \quad (\text{B4})$$

$$\mathcal{L}_4[A_4] = A_4(X)\phi^\mu\phi_{\mu\rho}\phi^{\rho\nu}\phi_\nu, \quad (\text{B5})$$

$$\mathcal{L}_5[A_5] = A_5(X)(\phi^\mu\phi_{\mu\nu}\phi^\nu)^2. \quad (\text{B6})$$

The functions  $G, G_2, G_3, A_i$  are arbitrary functions of  $X$ . This last point is assumed for simplicity; in principle these functions might also depend on  $\phi$ . In general, gravitational waves in this theory propagate at a speed different from

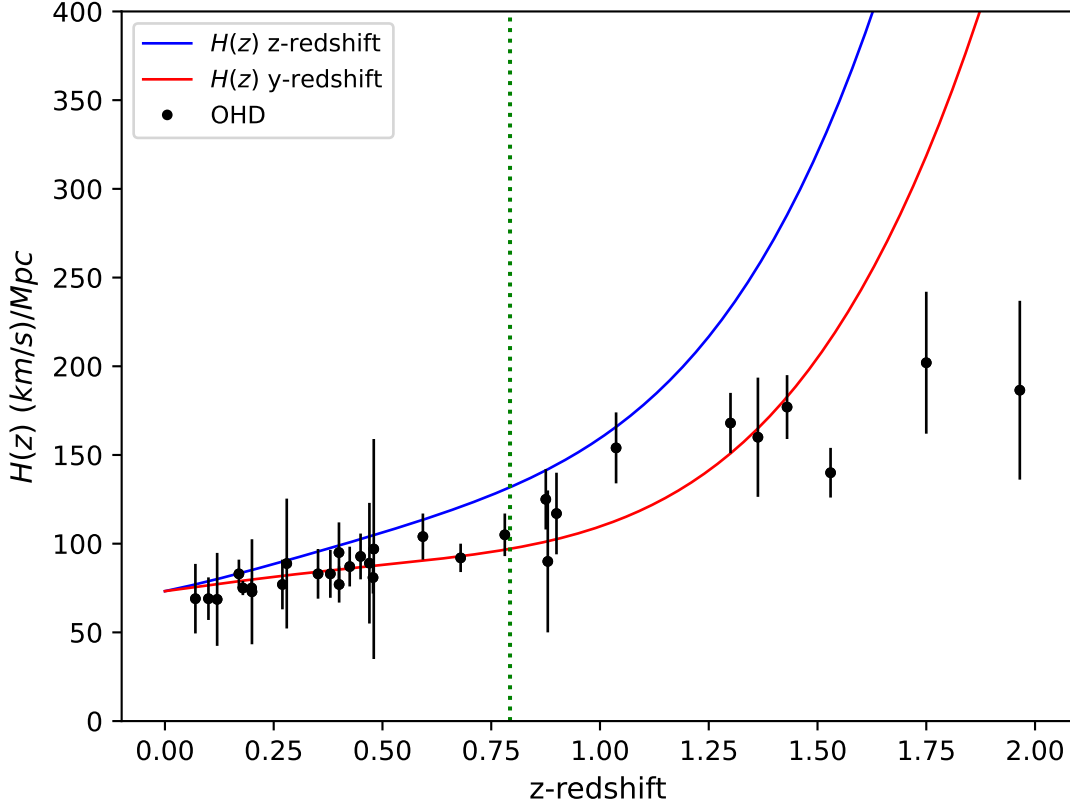


FIG. 8.  $H(z)$  in terms of the cosmographic parameters. The blue line represents the equation A10 in terms of cosmographic parameters obtained from table VI (in the  $z$ -redshift space), while the red line represents equation A10 in terms of cosmographic parameters obtained from the last column of table I (in the  $y$ -redshift space). The vertical green line represents the observational error bars from cosmic chronometers measurements compiled by [14].

that of electromagnetic waves. To avoid this, it is necessary to set  $A_1 = 0$ . Furthermore, the Ostrogradski ghost is avoided if  $A_2 = 0$  and [38]

$$\begin{aligned} A_4 &= -\frac{1}{8G}(8A_3G - 48G_X^2 - 8A_3G_XX + A_3^2X^2), \\ A_5 &= \frac{A_3}{2G}(4G_X + A_3X). \end{aligned} \quad (\text{B7})$$

Following [38], the free functions  $G, G_2, G_3$  and  $A_3$  are chosen as

$$G = \frac{M_P^2}{2} + \frac{c_4}{\Lambda_3^6}X^2, \quad G_2 = c_2X, \quad G_3 = \frac{c_3}{\Lambda_3^3}X, \quad A_3 = -\frac{8c_4}{\Lambda_3^6} - \frac{\beta}{\Lambda_3^6}. \quad (\text{B8})$$

With these choices, the model under consideration reduces to the covariant galileon of beyond Horndeski when  $\beta = 0$ .

The equations of motion are obtained by varying the Lagrangian with respect to the metric and scalar field, and then imposing the Ansatz that the line element describes a flat Friedmann-Robertson-Walker spacetime,

$$ds^2 = -dt^2 + a(t)^2(dr^2 + r^2d\theta^2 + r^2\sin^2\theta d\varphi^2), \quad (\text{B9})$$

and that the scalar field depends only on the time coordinate. As described in [38], this leads to three independent equations that contain up to fourth derivatives of the scalar field and second derivatives of the Hubble parameter. However; the spatial part of the field equations for the metric can be solved for  $H'$ , and after substituting the result

in the remaining equations one finds two second order equations that only contain  $\phi, \phi'$  and  $H$ . Then we look for numerical solutions to the two independent equations,

$$\begin{aligned}
0 = & \dot{\phi}^{12} \left\{ 8c_{24} \left[ \left( 9\beta\beta_{12} - 32c_4^2 \right) \ddot{\phi} + 24c_{34} \right] + 3\ddot{\phi} \left[ 9\beta^2\beta_{16}\beta_{20}\ddot{\phi}^2 + 72\beta c_{34}\beta_{16}\ddot{\phi} + 128c_{34}^2 \right] \right\} \\
& + 6\dot{\phi}^8 \left[ 2c_2 \left( \left( 3\beta^2 - 8c_4\beta_{12} \right) \ddot{\phi} + 16c_{34} \right) + \ddot{\phi} \left( 9\beta\beta_{16}\ddot{\phi} + 32c_{34} \right) \left( 2c_3 - \beta\ddot{\phi} \right) \right] - 32c_2\ddot{\phi} \\
& + 24\dot{\phi}^4 \left[ 4c_3\ddot{\phi}(c_3 - \beta\ddot{\phi}) + 2c_{23} - c_2(5\beta + 8c_4) \ddot{\phi} \right] + 36H^2\dot{\phi}^2 C_1^2 \left\{ 3\beta_{16}(\beta_{20}\dot{\phi}^4 - 2)\ddot{\phi} + 4c_3 C_1 \right\} \\
& - 12H\dot{\phi} C_1 \left\{ 4c_2 C_1(3\beta_{12}\dot{\phi}^4 + 2) + \left[ 8c_3 C_1(3\beta_{12}\dot{\phi}^4 - 2) + 3\beta\beta_{16}\dot{\phi}^4 \ddot{\phi}(3\beta_{20}\dot{\phi}^4 - 6) \right] \ddot{\phi} \right\}, \tag{B10}
\end{aligned}$$

$$0 = 3C_1^{-1}\beta^2\dot{\phi}^6 D_{20}\ddot{\phi}^2 + 24\beta c_3\dot{\phi}^6\ddot{\phi} + 4c_2\dot{\phi}^2 D_4 - 12H\dot{\phi}^3 \left( \beta D_{20}\ddot{\phi} + 4c_3 C_1 \right) + 12C_1 H^2 D_{20}, \tag{B11}$$

where

$$\begin{aligned}
C_1 &= 2c_4\dot{\phi}^4 + 1, \quad D_4 = 3\beta_4\dot{\phi}^4 + 2, \quad D_{20} = 3\beta_{20}\dot{\phi}^4 + 2, \\
\beta_{12} &= \beta + 4c_4, \quad \beta_{16} = \beta + 16c_4/3, \quad \beta_{20} = \beta + 20c_4/3, \\
c_{ij} &= c_i c_j, \tag{B12}
\end{aligned}$$

and we introduced the dimensionless quantities  $t \rightarrow M_P^{1/2} \Lambda_3^{-3/2} t, H \rightarrow M_P^{-1/2} \Lambda_3^{3/2} t, \phi \rightarrow M_P \phi$ .